Carrier-controlled anomalous Hall effect in an intrinsic ferromagnetic semiconductor

H. J. Trodahl, F. Natali, B. J. Ruck, and W. R. L. Lambrecht

Phys. Rev. B **96**, 115309 — Published 25 September 2017

DOI: 10.1103/PhysRevB.96.115309

Carrier-controlled anomalous Hall effect in an intrinsic ferromagnetic semiconductor

H.J. Trodahl, F. Natali, and B.J. Ruck
School of Chemical and Physical Sciences and The MacDiarmid Institute for Advanced Materials and Nanotechnology, Victoria University of Wellington, PO Box 600, Wellington 6140, New Zealand

W.R.L. Lambrecht
Department of Physics, Case Western Reserve University, Cleveland, Ohio 44106-7079, USA

The intrinsic ferromagnetic semiconductor GdN offers a unique opportunity to separate the anomalous and ordinary contributions to the Hall effect, and to investigate the strength of the anomalous Hall effect (AHE) as a function of carrier concentration and relaxation time. The data show an AHE that is inversely proportional to the carrier concentration n in a single spin channel. There is no dependence at all on the relaxation time τ, rather than the usual τ^1 or τ^2 dependencies predicted by conventional mechanisms. However, the n and τ dependencies are identical to those of the ordinary Hall effct (OHE), which suggests a semiclassical wave-packet description of an intrinsic AHE contribution that ultimately provides a *quantitative* agreement with the data.

PACS numbers: 72.25.Dc, 73.50.Jt 75.50.Pp

I. INTRODUCTION

The anomalous Hall effect (AHE) is a current-transverse voltage proportional to the magnetisation of ferromagnetic conductors that has been recognised for more than a century.[1] For more than half a century the effect has been recognised as resulting from the spin-orbit (SO) interaction, which deflects in opposite senses the paths of spin-up and spin-down electrons.[2] The experimental literature is overwhelmingly focused on ferromagnetic metals, in which it has been common to investigate the transverse Hall resistivity (ρ_{xy}) as a function of the longitudinal resistivity (ρ_{xx}).[3–5]

Three competing mechanisms are proposed for the AHE: (1) a side-step scattering at each impurity scattering event, (2) a skew scattering from the same impurities and (3) an intrinsic assymetry resulting from the SO interaction at host ions.[3] They are usually separated by their dependence on the scattering frequency $\gamma = \tau^{-1}$, relying on the approximately fixed carrier concentration in metals to permit the use of the longitudinal resistivity as a proxy for γ.[3] An independent control of the carrier concentration and relaxation time in semiconductors offers the opportunity to separate the influences of the two parameters, but a paucity of suitable intrinsic ferromagnetic semiconductors has so far prevented such a study. The recent recognition of the rare-earth nitrides as a series of epitaxy-compatible intrinsic ferromagnetic semiconductors relieves that bottleneck.[6–8] Here we report a study of the AHE and the ordinary Hall effect (OHE) in films of GdN, the prototypical rare-earth nitride, with a wide range of carrier concentrations and relaxation times.

The rare-earth nitrides condense into the NaCl structure, with a lattice constant close to 0.5 nm.[9] Their wide-ranging magnetic and coupled magnetic-electronic responses have seen them included in a number of device structures.[10–13] The series includes at least one superconducting member,[14] and *ab initio* calculations support the suggestion that they may show both ferroelectric[15] and topological insulator[16] phases. GdN lies in the center of the series with a purely spin magnetic moment of 7 Bohr magnetons (μ_B) per primitive cell that is sited primarily in the Gd^{3+} $4f$ shell.

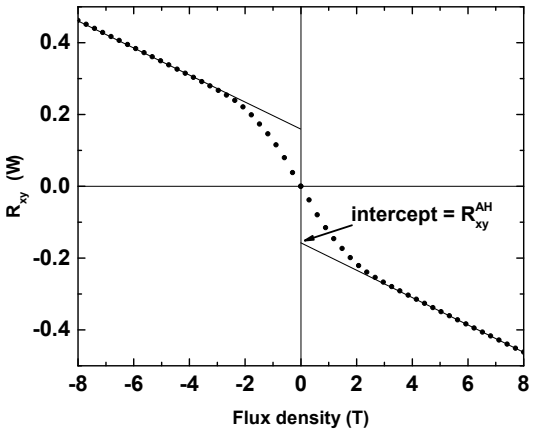

FIG. 1. Typical Hall data in GdN. Above 2.1 T the field dependence is linear with a slope of the OHE, while the zero-field intercept gives the saturation value of the AHE.

Electron transport occurs in the $5d$ conduction band that is populated by nitrogen-vacancy (V_N) donors.[17,18] A ferromagnetic $5d$-$4f$ exchange interaction ensures that the $5d$ alignment follows the $4f$ alignment, thus retaining the close connection between the magnetisation and the spin imbalance in the conduction band. For the Hall geometry in thin films the shape anisotropy dictates that the magnetisation rises linearly with an applied field B until the magnetisation saturates above $B = 4\pi M_{sat} \approx 2.1$ T for the large magnetisation of GdN, where M_{sat} is the saturation magnetisation. Above that field the AHE

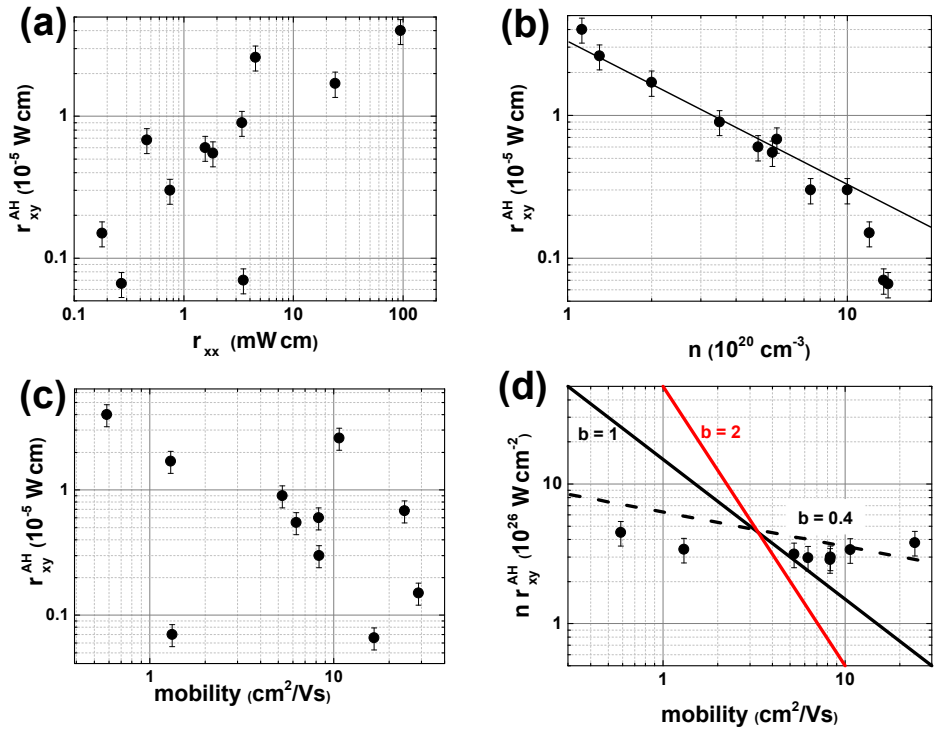

FIG. 2. (Color online) The amplitude of the AHE in donor-doped GdN as a function of (a) the resistivity, (b) the electron concentration, (c) the electron mobility and (d) the mobility after correcting for the concentration influence. It is clear that there is no correlation with the mobility, but as highlighted by the line in (b) there is rather an excellent, tightly-defined inverse correlation with the electron concentration for the electron concentration below 10^{21} cm^{-3}.

is saturated, and the net Hall effect then increases with the OHE, as seen in the data of Figure 1.[6,19,20] With such a simple field dependence the carrier concentration can be determined from the slope at high fields, and the AHE magnitude is given by the extrapolation to zero field. Note that the coercive field is so small in GdN ($\approx$ 0.01 T) as to be irrelevant at the scale of Figure 1.[21]

II. EXPERIMENTAL DETAILS

The GdN films used in the present work were grown to thickness of 50-150 nm in four different growth chambers. They comprise a mixture of epitaxial and polycrystalline films. The films were grown at 0.5-1.0 nm s^{-1} in the presence of $\approx 10^{-4}$ mbar of pure N_2 or ammonia. They had carrier concentrations controlled by varying the V_N concentration[6,20,22] and by the introduction of Mg as an acceptor.[23] The relaxation time was limited by a mixture of point defects (e.g., V_N, Mg dopants) and grain boundaries, so as seen below it is not simply related to the carrier concentration.

Magneto-transport measurements at 2-300 K and in fields to $\pm$8 T were performed in a Quantum Design PPMS. The results all conform to the pattern seen in Figure 1, with both the ordinary and the anomalous contributions negative and the knee corresponding to the shape-anisotropy limit at $\approx$2.1 T.[20] For the present purpose we focus on temperatures of $\leq$ 20 K, well below the GdN Curie temperature of 50-70 K,[6] to ensure that the magnetization is within a few percent of its zero-temperature saturated value.

III. RESULTS AND DISCUSSION

A. Carrier concentration and mobilty dependencies

The carrier concentrations and AHE magnitudes from a wide range of GdN films, along with the mobility determined by resistivity data, display a remarkably consistent correlation. In Figure 2(a) the AHE magnitudes are plotted against the resistivity, as is the common presentation for ferromagnetic metals. There is a loosely-defined

correlation which in metals would suggest that the AHE is inversely proportional to the electron relaxation time, or equivalently the mobility.[3] However, in these semiconductor films there is a simple inverse dependence on the carrier concentration [Figure 2(b)] and no dependence at all on the relaxation time [Figure 2(c)].

The lack of any systematic AHE dependence on the electron mobility in the present data set is at odds with conventional expectations, so it is essential to understand how strongly the data support that lack. Figure 2(c) shows a widely scattered pattern, so we show also in Figure 2(d) ρ_{xy}^{AH} after correction for the inverse carrier concentration dependence. The data span less than a factor of 1.5 (i.e., $\pm 20\%$) as the mobility changes by two orders of magnitude. The evidence for a lack of scattering dependence is exceedingly strong.

The common $1/n$ dependence of the ordinary and anomalous contributions to the Hall effect ensure that the two contributions scale, that the ratio between them is independent of the carrier concentration. In terms of their resistivities, the line in Figure 2(b) defines

$$\rho_{xy}^{AH} = \frac{2.2 \times 10^{-5}}{n}\ \Omega\text{cm} = \rho_{xy}^{OH}\frac{5\ \text{T}}{B}. \quad (1)$$

Thus for carrier concentration less than 10^{21} cm^{-3} the OHE is equal to the AHE at $B = 5$ T, as already seen in Figure 1.

In the following sections we focus first on the correlation between the AHE and the carrier concentration, which agrees well with with a purely majority-spin transport channel seen in the computed band structure. We then move to discuss the lack of the relaxation-time dependence that is in such strong direct disagreement with the three common mechanisms for the AHE.

B. Filling the majority-spin band

The anomalous Hall conductivity σ_{xy}^{AH} has opposite contributions from the two spin-oriented electrons; it follows the difference $(n_\uparrow - n_\downarrow)$ between the concentration of spin up $(n_\uparrow)$ and spin down $(n_\downarrow)$ electrons, whereas the longitudinal conductivity σ_{xx} follows the sum $(n_\uparrow + n_\downarrow)$. The measurements correspond to the resistivity, $\rho_{xy} = \sigma_{yx}/\sigma_{xx}^2$ for $\sigma_{yx} \ll \sigma_{xx}$, giving a concentration dependence of $(n_\uparrow - n_\downarrow)/(n_\uparrow + n_\downarrow)^2$ for the anomalous Hall resistivity ρ_{xy}^{AH}. Thus a signature of a single-spin channel, with $n_\downarrow = 0$, is that the AHE, like the OHE, is inversely proportional to the carrier concentration. This is exactly the dependence in moderately-doped GdN seen in Figure 2(b); evidently only one spin state populates the conduction band of GdN until there are 10^{21} cm^{-3} carriers. At larger concentration the minority-spin band begins to fill, reducing the relative spin imbalance to reduce the AHE below the $1/n$ extrapolation.

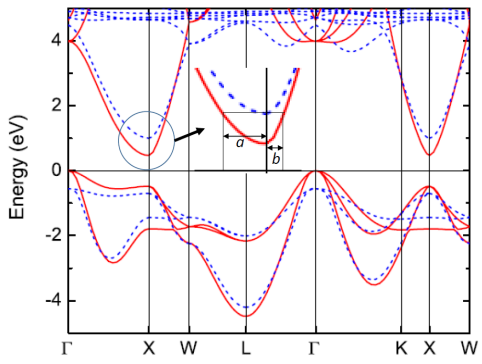

FIG. 3. (Color online) LSDA+U-calculated band structure of ferromagnetic GdN (from Ref. [8]). The solid red (dashed blue) lines represent the majority (minority) spin bands. The expanded view of the conduction-band minimum identifies the semimajor (a) and semiminor (b) axes of the majority-spin prolate spheroid immediately before increasing the carrier concentration to start filling the minority-spin pocket.

The LSDA+U computed band structure for GdN shows three prolate-spheroid electron pockets at the X points (see Figure 3), with a spin splitting of ≈ 1 eV.[8,24] The concentration at which the Fermi energy reaches the minority-spin conduction band is determined by the volume of the majority-spin pockets at the Fermi energy corresponding to the bottom of the minority-spin pockets. The semi-axes a and b of the maximum-volume spheroids are noted in Figure 3, in terms of which the maximum purely majority-spin filling is

$$\frac{1}{(2\pi)^3}\frac{4\pi}{3}ab^2. \quad (2)$$

The dimensions shown in Figure 3 give a carrier concentration of 3×10^{20} cm^{-3}, so that the net purely majority-spin electron concentration in the three X-point pockets is $\sim 10^{21}$ cm^{-3}, in excellent agreement with the data. For lower concentration the conduction channel is purely of majority spin, as the AHE data suggest.

C. Semiclassical treatment of the AHE

Theoretical AHE descriptions are firmly focused on the dependence of the AHE on the scattering frequency γ, described in terms of an exponent defined by

$$\rho_{xy}^{AH} \propto \gamma^\beta \quad (3)$$

The competing AHE scenarios are characterised as: (i) skew scattering by impurities ($\beta = 1$), (ii) side jump scattering events ($\beta = 2$) and (iii) the intrinsic Berry

phase description ($\beta = 2$).[3] The expected run of the AHE is shown by the lines in Figure 2(d); the data disagree exceedingly strongly with them both. However, there is a large body of data in a strongly disordered regime showing a superlinear dependence of the anomalous Hall conductivity σ_{xy}^{AH} on the longitudinal conductivity σ_{xx}

$$\sigma_{xy}^{AH} \propto \sigma_{xx}^{\alpha}; \quad 1 \leq \alpha \leq 2; \;\; 1 \geq \beta \geq 0. \tag{4}$$

The phenomenon has been modelled by Onoda et al.,[4] where the exponent $\alpha \approx 1.6$ ($\beta \approx 0.4$) is found for $\rho_{xx} \geq 0.5$ mΩcm corresponding to the range in these GdN films. We thus show the expected dependence in Figure 2(d). The GdN data, with $\beta = 0$, does not fit to any of these scenarios. Furthermore the lack of any dependence on the various differing scattering centres in the wide range of samples suggests that the details of defect scattering are unimportant and encourages a consideration of an intrinsic mechanism for the observed AHE. We thus proceed on that path.

The spin-orbit interaction necessarily introduces a term in the Hamiltonian that shows the full translational symmetry of the crystal, whose primary effect is mixing among the various bands, as is of central importance in the Berry-phase description of the intrinsic AHE.[25] However, within the semiclassical description of electron transport one notices that, in addition to the periodic terms that are absorbed into the effective mass, an electron traversing the crystal experiences also a transverse force with a finite volume average, which we now treat within the semiclassical model.

Our treatment is based on the Boltzmann equation, for which the solutions are textbook material.[26–28] In the presence of a magnetic field there is a velocity-transverse Lorentz force on each electron that introduces a transverse acceleration proportional to the electron velocity, which in Gaussian units is given by

$$\dot{\mathbf{v}} = \frac{e}{m^* c} \mathbf{v} \times \mathbf{B}, \tag{5}$$

where c is the speed of light. This in turn leads to a deflection of the path within the wave-packet description of the electron at an angular rate given by

$$\dot{\theta} = \omega_{\rm c} = \dot{v}_{\perp}/v = \frac{eB}{m^* c}, \tag{6}$$

where $\dot{v}_{\perp}$ is the component of acceleration perpendicular to the velocity. For the quadratic electron dispersion at the conduction-band minimum the electron paths are deflected through an angle $\omega_{\rm c}\tau$ ($\omega_{\rm c}$ the cyclotron frequency) under the influence of the Lorentz force. For short relaxation times, ($\omega_{\rm c}\tau \ll 1$),

$$\sigma_{xy} = \sigma_{xx}\omega_{\rm c}\tau, \tag{7}$$

which imposes the τ^2 dependence on σ_{xy}. Inverting to the resistivity tensor yields an ordinary Hall resistivity

$$\rho_{xy} = \rho_{xx}\omega_{\rm c}\tau. \tag{8}$$

The resistivity ρ_{xx} depends inversely on τ to give a Hall resistivity that is independent of scattering.

Turning now to the spin-orbit interaction, the magnetic field sensed by an electron moving with velocity $\mathbf{v}$ through the electric field in a crystal is given by the usual relativistic transformation

$$\mathbf{B} = -\frac{1}{c}\mathbf{v} \times \mathbf{E}. \tag{9}$$

Note that Equation 9 assumes a nonrelativistic velocity, $\frac{v}{c} \ll 1$. The electron, with magnetic moment $\boldsymbol{\mu}$, experiences a force

$$\mathbf{F} = \boldsymbol{\nabla}(\boldsymbol{\mu} \cdot \mathbf{B}). \tag{10}$$

Within the semiclassical picture the electron is represented by a Bloch wave packet traveling with the group velocity. Taking the volume average of the product of the force and the square of the wave function, which reduces trivially to the integral over a primitive cell, we have:

$$\mathbf{F} = -\frac{1}{c}\int d^3r \boldsymbol{\nabla}[\boldsymbol{\mu} \cdot (\mathbf{v} \times \mathbf{E})] \, |u_{\mathbf{k}}|^2. \tag{11}$$

As usual the Bloch-wave phase factor does not contribute to the function $|u_{\mathbf{k}}|^2$, which then has the full translation and point symmetry of the lattice. The equation assumes that $|u_{\mathbf{k}}|^2$ is normalised within the primitive cell.

Deep in the ferromagnetic phase the magnetic moment of a conduction-band electron can be represented as $\mu_B \hat{\mathbf{z}}$, and selecting the in-plane (i.e., magnetic-moment transverse) velocity to be along x,

$$\mathbf{F} = -\frac{\mu_B v_x}{c}\int d^3r \boldsymbol{\nabla} E_y \, |u_{\mathbf{k}}|^2. \tag{12}$$

The x and z components of $\boldsymbol{\nabla} E_y$ are odd about the centers of inversion in the crystal, and $|u_{\mathbf{k}}|^2$ is even, so that the only component of the force is transverse to both the magnetic moment and the velocity, and it has the magnitude

$$F_y = -\frac{\mu_B v_x}{c}\int d^3r \frac{\partial E_y}{\partial y} \, |u_{\mathbf{k}}|^2 \tag{13}$$

which drives a transverse acceleration and redirects the field-normal velocity at a rate

$$\omega_{so} = \frac{\dot{v}_y}{v_x} = -\frac{\mu_B}{m^* c}\int d^3r \frac{\partial E_y}{\partial y} \, |u_{\mathbf{k}}|^2. \tag{14}$$

Under the cubic point symmetry of GdN, the three coordinates return identical integrals, so that

$$\omega_{so} = \frac{-\mu_B}{3m^*c}\int d^3r \boldsymbol{\nabla}\cdot\mathbf{E}\,|u_{\mathbf{k}}|^2 = \frac{-4\pi\mu_B}{3m^*c}\int d^3r\rho(\mathbf{r})\,|u_{\mathbf{k}}|^2. \quad (15)$$

Here $\rho(\mathbf{r})$ is the charge density of all nuclei and electrons within the unit cell. The form of the deflection is entirely analogous to the Lorentz-force deflection for which the Boltzmann equation then leads to the mobility independent AHE ($\beta = 0$) in common with the conventional Hall effect.[26,27] For the single-spin channel of GdN the Boltzmann-equation solution gives a clear relationship between the diagonal and off-diagonal elements in the resistivity:[27,28]

$$\rho_{xy} = \rho_{xx}(\omega_c\tau + \omega_{so}\tau), \quad (16)$$

$$\rho_{xx} = \frac{m^*}{ne^2\tau}, \quad (17)$$

$$\omega_c = \frac{eB}{m^*c}. \quad (18)$$

Finally the ratio of AHE to OHE is given by

$$\frac{\rho_{xy}^{AH}}{\rho_{xy}^{OH}} = \frac{\omega_{so}}{\omega_c} = \frac{-4\pi\mu_B}{3eB}\int d^3r\rho(\mathbf{r})\,|u_{\mathbf{k}}|^2. \quad (19)$$

One expects that both terms in the integrand are even about a center of inversion, so simple symmetry arguments are not helpful to establish a zero integral. $\rho(\mathbf{r})$ is the charge density in an undoped GdN unit cell, including all charges of the Gd^{3+} and N^{3-} ions. The net charge within a unit cell is necessarily zero, but the conduction band consists of nearly pure Gd $5d$ character, which features zero weight at the Gd nucleus, the site of the single largest contribution to the charge. The intergral then involves the remaining -eZ$_{\rm Gd}$ with Z$_{\rm Gd}$ = 64, though the electronic charge from the most tightly bound core states will also be diminished by the vanishing weight of the $5d$ wave function near the Gd nucleus. Thus as a first approximation one expects the integral to return somewhat less that $\frac{64e}{V}$ for a unit cell volume V, so that

$$\int d^3r\rho(\mathbf{r})\mid u_{\mathbf{k}}\mid^2 = -\eta\frac{64e}{V} \quad (20)$$

and

$$\frac{\omega_{so}}{\omega_c}B = \eta\frac{256\pi\mu_B}{3V} \quad (21)$$

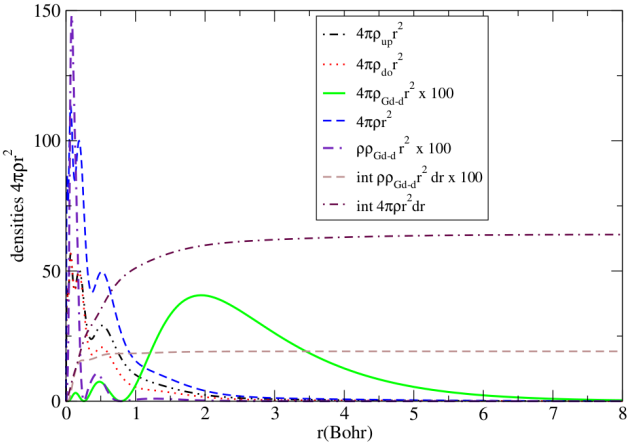

FIG. 4. (Color on-line) Calculation of the integral in Eq. 20 and its contributions.

with $\eta < 1$. With the GdN cell volume ($V = 3.1\times 10^{-23}$ cm^3),

$$\frac{\omega_{so}}{\omega_c}B = \eta 7.9\times 10^4 \text{ G} = \eta 7.9 \text{ T}. \quad (22)$$

Recalling that the ratio $\frac{\omega_{so}}{\omega_c}$ is 1.0 at 5 T, one finds that $\eta = 0.6$, an entirely reasonable result.

A first-principles estimate of the integral in Eq. 20 can be determined as follows. The Bloch state at the conduction band minimum $u_{\mathbf{k}}$ is essentially a d_{xy} state when the conduction band minimum is considered at $k_X = [0,0,1]2\pi/a$. Thus the integral over angles in Eq. 20 reduces to the spherical harmonic normalization integral and we are left with

$$\int_0^s r^2 dr\rho(r)R_d(r)^2 \quad (23)$$

where $R_d(r)$ is the radial part of the Gd-d function and s is the size of a sphere around the Gd atom. We replace it by the free atom Gd-d radial wave function calculated within the local density approximation for simplicity. The upper limit is not very crucial because, as we will see, most of the integral comes from the inner part of the sphere and is well converged within a touching muffin-tin sphere around the Gd site. Fig. 4 shows the behavior of the relevant functions and the integral.

It shows the up and down spin contributions to the total charge density $4\pi\rho(r)r^2$ which is seen to integrate to 64. The Gd-partial contribution $4\pi\rho_{Gd-d}r^2 = 4\pi R_d^2(r)r^2$ is shown by the green line, multiplied by a factor 100 to make it visible. Although this function is seen to have its maximum at about 2 a_0 and extend till about 7 a_0 the relevant integral shown by the dashed brown line is seen to converge to a value of about 0.19 within about 1 a_0. The volume of the unit cell, $V = 208a_0^3$ corresponds to a density of $n = 64/208 = 0.30a_0^{-3}$. Thus our calculated η factor is 0.19/30 = 0.63 in excellent agreement with the above experimental estimate.

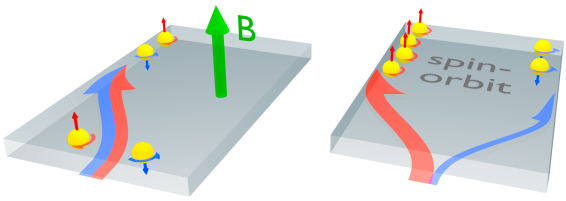

FIG. 5. (Color online) Sketch of the electron trajectories leading to the ordinary (left) and anomalous (right) Hall effects. The circulating arrows represent the spin angular momentum sense, and the up/down arrows give the direction of the magnetic dipole moments. The sketch is drawn assuming that (i) the favored spin magnetic moment is parallel to the magnetic field and (ii) a magnetic-moment up electron is deflected to the left, for which the OHE and AHE share a common sign.

Finally we note that the common negative sign between the OHE and AHE is exactly as expected, based on the electron doping into a band where the magnetic dipole moments of the carriers align with the applied magnetic field. For the velocity $\mathbf{v}$ along $\hat{\mathbf{x}}$ and the magnetic field along $\hat{\mathbf{z}}$ an electron is deflected toward the left, i.e., toward positive $\hat{\mathbf{y}}$. The resulting trajectories are illustrated in Figure 5.

The data in the present paper clearly relate closely to the strong scattering limit within the Berry-phase description of the intrinsic AHE.[3,4,25] The scattering dependence of σ_{xy}^{AH} predicted[4] as proportional to $\tau^{1.6}$ appears in the present semiclassical model to follow the measured dependence on τ^2. Furthermore the present model returns a magnitude in quantitative agreement with the data. The inference is that the intrinsic σ_{xy}^{AH} is reduced at scattering rates $\tau^{-1} \geq \omega_{so}$, thereafter following a τ^2 dependence.

IV. SUMMARY

We have reported measurements of the anomalous Hall effect in GdN. The results display a very simple field dependence that permits a clear separation of the ordinary and anomalous Hall resistances. Furthermore, both the carrier concentration and the scattering rate are amenable to control in this intrinsic ferromagnetic semiconductor, which has provided a unique opportunity for an unambiguous investigation of the dependence of the anomalous Hall effect on these two parameters. There is an especially simple inverse dependence on the carrier concentration that is easily understood as signalling that the current carriers reside in a majority spin band; the minority-spin band remains unoccupied until the carrier concentration reaches 10^{21} cm^{-3}. That carrier concentration coincides with the prediction based on an LSDA+U band structure calculation, confirming the utility of the band structure and highlighting GdN as a single-spin-channel semiconductor.

The measurements show a lack of any dependence on the carrier mobility, or equivalently electron relaxation time, at variance with currently formulated mechanisms for the anomalous Hall effect. We provide an inclusion of the intrinsic spin-orbit interaction within a semiclassical model that is in excellent agreement with the entire data set, and suggest that it represents the strong-scattering limit of the Berry-phase intrinsic AHE.

ACKNOWLEDGMENTS

The authors are grateful to Ulrich Zülicke and Michele Governale for much excellent discussion concerning the conventional theoretical description of the AHE, and to a large number of students, postdoctoral fellows and collaborators for film growth and transport measurements. The research was supported by the New Zealand Marsden Fund (Grant No.s 13-VUW-1309, 08-VUW-1309). The MacDiarmid Institute is supported under the New Zealand Centres of Research Excellence Programme. W.L was supported by the U.S. Department of Energy Basic Energy Sciences, under grant No. DE-SC0008933.

[1] E. H. Hall, Philos. Mag. **12**, 157 (1881).
[2] R. Karplus and J. M. Luttinger, Phys. Rev. **95**, 1154 (1954).
[3] N. Nagaosa, J. Sinova, S. Onoda, A. H. MacDonald, and N. P. Ong, Rev. Mod. Phys. **82**, 1539 (2010).
[4] S. Onoda, N. Sugimoto, and N. Nagaosa, Phys. Rev. B **77**, 165103 (2008).
[5] D. Yue and X. Jin, J. Phys. Soc. Jpn **86**, 011006 (2017).
[6] F. Natali, B. Ruck, N. Plank, H. Trodahl, S. Granville, C. Meyer, and W. Lambrecht, Prog. Mater. Sci. **58**, 1316 (2013).
[7] S. Granville, B. J. Ruck, F. Budde, A. Koo, D. J. Pringle, F. Kuchler, A. R. H. Preston, D. H. Housden, N. Lund, A. Bittar, G. V. M. Williams, and H. J. Trodahl, Phys. Rev. B **73**, 235335 (2006).
[8] H. J. Trodahl, A. R. H. Preston, J. Zhong, B. J. Ruck, N. M. Strickland, C. Mitra, and W. R. L. Lambrecht, Phys. Rev. B **76**, 085211 (2007).
[9] F. Hulliger, *Handbook on the Physics and Chemistry of the Rare Earths*, Vol. 4 (North Holland, 1979) pp. 153–236.
[10] H. Warring, H. J. Trodahl, N. O. V. Plank, F. Natali, S. Granville, and B. J. Ruck, Phys. Rev. Appl. **6**, 044002 (2016).
[11] P. K. Muduli, A. Pal, and M. G. Blamire, Phys. Rev. B

89, 094414 (2014).
[12] H. Yoshitomi, S. Kitayama, T. Kita, O. Wada, M. Fujisawa, H. Ohta, and T. Sakurai, Phys. Rev. B **83**, 155202 (2011).
[13] S. Krishnamoorthy, T. F. Kent, J. Yang, P. S. Park, R. C. Myers, and S. Rajan, Nano Lett. **13**, 2570 (2013).
[14] E.-M. Anton, S. Granville, A. Engel, S. V. Chong, M. Governale, U. Zülicke, A. G. Moghaddam, H. J. Trodahl, F. Natali, S. Vézian, and B. J. Ruck, Phys. Rev. B **94**, 024106 (2016).
[15] H. M. Liu, C. Y. Ma, C. Zhu, and J.-M. Liu, J. Phys.: Condens. Matter **23**, 245901 (2011).
[16] Z. Li, J. Kim, N. Kioussis, S.-Y. Ning, H. Su, T. Iitaka, T. Tohyama, X. Yang, and J.-X. Zhang, Phys. Rev. B **92**, 201303 (2015).
[17] F. Natali, B. J. Ruck, H. J. Trodahl, D. L. Binh, S. Vezian, B. Damilano, Y. Cordier, F. Semond, and C. Meyer, Phys. Rev. B **87**, 035202 (2013).
[18] A. Punya, T. Cheiwchanchamnangij, A. Thiess, and W. R. L. Lambrecht, *Symposium I Magnetism and Correlated Electronic Structure of NitridesRare-Earth and Transition Metals as Constituents and Dopants*, MRS Proceedings, **1290**, 4 (2011).
[19] M. Scarpulla, C. Gallinat, S. Mack, J. Speck, and A. Gossard, J. Cryst. Growth **311**, 1239 (2009).
[20] F. Natali, N. Plank, J. Galipaud, B. Ruck, H. Trodahl, F. Semond, S. Sorieul, and L. Hirsch, J. Cryst. Growth **312**, 3583 (2010).
[21] B. M. Ludbrook, I. L. Farrell, M. Kuebel, B. J. Ruck, A. R. H. Preston, H. J. Trodahl, L. Ranno, R. J. Reeves, and S. M. Durbin, J. Appl. Phys. **106**, 063910 (2009).
[22] N. O. V. Plank, F. Natali, J. Galipaud, J. H. Richter, M. Simpson, H. J. Trodahl, and B. J. Ruck, Appl. Phys. Lett. **98**, 112503 (2011).
[23] C.-M. Lee, H. Warring, S. Vezian, B. Damilano, S. Granville, M. Al Khalfioui, Y. Cordier, H. J. Trodahl, B. J. Ruck, and F. Natali, Appl. Phys. Lett. **106**, 022401 (2015).
[24] P. Larson, W. R. L. Lambrecht, A. Chantis, and M. van Schilfgaarde, Phys. Rev. B **75**, 045114 (2007).
[25] D. Xiao, M.-C. Chang, and Q. Niu, Rev. Mod. Phys. **82**, 1959 (2010).
[26] N. F. Mott and H. Jones, *The Theory of the Properties of Metals and Alloys* (Clarendon Press, 1936).
[27] J. M. Ziman, *Electrons and Phonons* (Oxford University Press, 1960) pp. 483–500.
[28] F. J. Blatt, *Physics of Electronic Conduction in Solids* (McGraw-Hill, 1968).